Available online at www.sciencedirect.com
SCIENCE DIRECT®

C. R. Mecanique 333 (2005) 389–395

COMPTES RENDUS
MECANIQUE

http://france.elsevier.com/direct/CRAS2B/

An approximate solution to the problem of cone or wedge indentation of elastoplastic solids

Guillaume Kermouche [a], Jean-Luc Loubet [b], Jean-Michel Bergheau [a,*]

[a] *LTDS, UMR 5513 CNRS/ECL/ENISE, 58, rue Jean-Parot, 42023 Saint-Etienne cedex 2, France*
[b] *LTDS, UMR 5513 CNRS/ECL/ENISE, 36, avenue Guy-de-Collongue, 69134 Ecully cedex, France*

Received 1 February 2005; accepted 29 March 2005

Presented by Jean-Baptiste Leblond

Abstract

The model developed in this Note makes it possible to determine the value of the mean indentation pressure usually named hardness from the elastoplastic properties of materials and also the shape of the cone or that of the wedge. The approximation rests upon the definition of a linear elastic solid which has the same indentation pressure as the material actually indented. Cases of cone and wedge indentation are studied. A method to determine the uniaxial stress–strain curve of materials from indentation tests is given. The results are validated using finite element simulations. ***To cite this article: G. Kermouche et al., C. R. Mecanique 333 (2005).***

Résumé

Solution approchée du problème de l'indentation cônique et diédrique de matériaux élastoplastiques. Le modèle développé dans cette Note permet de déterminer la valeur de la pression moyenne d'indentation (habituellement dénomée dureté) à partir des propriétés élastoplastiques des matériaux. L'approximation développée repose sur la définition d'un solide élastique linéaire dont la pression moyenne d'indentation est la même que celle du matériau réellement indenté. Une méthode d'identification de la courbe contrainte-déformation uniaxiale à partir d'essais d'indentation est proposée. Les résultats sont ensuite validés à l'aide de calculs par éléments finis. ***Pour citer cet article : G. Kermouche et al., C. R. Mecanique 333 (2005).***

Keywords: Solids and structures; Cone Indentation; Elastoplasticity; Representative stress; Identification method

Mots-clés : Solides et structures ; Indentation cônique ; Elastoplasticité ; Contrainte représentative ; Méthode d'identification

* Corresponding author.
E-mail addresses: guillaume.kermouche@enise.fr (G. Kermouche), jean-luc.loubet@ec-lyon.fr (J.-L. Loubet), jean-michel.bergheau@enise.fr (J.-M. Bergheau).

1631-0721/$ – see front matter
doi:10.1016/j.crme.2005.04.001

1. On indentation tests

The understanding of the indentation of solids is very important to measure the mechanical properties of surfaces. The instrumented indentation method makes it possible to measure continuously the load applied on the indenter as a function of the penetration depth. Thus, the study of the load-penetration curve can be used to determine mechanical properties even when the penetration is very small. The indentation of isotropic elastoplastic material has been widely investigated over the past few years [1–4] and many laws from experimental studies and simplified models have been proposed. Recently, the development of nanoindentation techniques [5, 6] has made it possible to finely characterize the mechanical properties of surfaces. The aim of this study is to propose a new approximate solution of the indentation of elastoplastic materials using a rigid cone or a rigid wedge.

Using an empirical approach based on experiments on metals, Tabor [1] explains that the real definition of hardness is the mean pressure under load. Assuming that the principle of geometric similarity can be applied to elastoplastic materials indented by sharp indenters (cone, wedge, Berkovitch, Vickers, etc.), the mean pressure is constant during the penetration. The principle of geometric similarity (PGS) has been described by many authors [1,7,4] and states that if two indentations are made of the same geometric shapes, then, whatever their size, the strain and stress distributions around the indentation will be geometrically similar. For cone indentation of half-space, the PGS means that stress and strain fields can be written as functions of some reduced coordinates $X = r/a(t)$ and $Z = z/a(t)$ where r and z are polar coordinates and $a(t)$, the contact radius at time t.

$$\sigma_{ij}(r,z,t) = \Sigma_{ij}(X,Z) \quad \text{and} \quad \varepsilon_{ij}(r,z,t) = E_{ij}(X,Z) \tag{1}$$

Eq. (1) leads to a contact pressure function of reduced coordinates. Hence the mean pressure does not depend on the applied load. There is a close resemblance between problems where geometric similarity is maintained and problems of steady motion. A representative stress σ_r and a representative strain ε_r characterizing the stress and strain distributions (Σ_{ij} and E_{ij}) corresponding to each other on the uniaxial stress–strain curve can be defined.

Tabor's suggestion [1] is to relate a representative stress to the mean pressure $\sigma_r = p_m/3$ and a representative strain to the shape of the indenter $\varepsilon_r = 0.2\tan(\beta)$ with β the angle from the face of the indenter to the surface. Hence the uniaxial stress–strain curve can be obtained in a non destructive way using indentation tests. Using similarity principles, Hill et al. [3,7] and Storakers et al. [8] have shown that these empirical results are valid for rigid plastic materials with power law hardening. It has been confirmed by the finite element study of Larsson et al. [9]. However, when elastic properties have to be taken into account, Tabor's relationships are no longer valid. Using the analytical solution of the expansion of an elastoplastic spherical cavity under a hydrostatic pressure and assuming that this result can be applied to model cone indentation tests, Johnson [10] proposed an expression where the mean pressure (or hardness) is related to the yield stress and elastic properties. Using dimensional analysis and scaling relationships, Cheng and Cheng [4] have applied these methods to the understanding of the effects of the mechanical properties on indentation results. They have shown in particular that for given elastic properties, E and ν, multiple choices of the plastic parameters – yield stress, strain hardening exponent – are possible, which produce the same hardness value. Several studies have been made to compare the force penetration curve obtained experimentally and also using numerical simulations [11,4]. Recently, several authors have established dimensionless functions for a wide range of material properties using intensive finite element simulations [12]. These functions express the indentation load as a function of mechanical and geometrical properties and have been mainly developed for sharp indentations. Then they used several algorithms to identify plastic parameters [13,14]. The most important drawback of such approaches is that the strain hardening curve must be known. Moreover, results are not always stable depending on elastoplastic properties and regulation methods have to be applied [15].

2. A new approximation of wedge and cone indentation

In Sections 2, 3 and 4, the constitutive elastoplastic equations are based on the classical rate independent Prandtl–Reuss equations for von Mises plasticity with isotropic hardening. Let us introduce the ratio between the mean pressure p_m and the representative stress σ_r, $\gamma = p_m/\sigma_r$. γ depends on β and on the elastoplastic properties of the indented material. For linear elastic solids, $\gamma = \gamma_e$ depends only on elastic properties and on β. For rigid perfectly plastic materials, σ_r is equal to the yield stress $Y \cdot \gamma = \gamma_p$ depends only on β (Hill [16], Lockett [17]).

For wedge and cone indentation of linear elastic half-space, the expression of the mean pressure is the same. It is given by (Love [18]):

$$p_m = \frac{1}{2}\frac{E}{1-\nu^2}\tan(\beta) \tag{2}$$

Let us now consider representative stress and strain definitions in this case. On a uniaxial tensile test, the stress is related to the strain by the $\sigma = E\varepsilon$ equation. Following the work of Tabor [1], the representative stress of the indentation test is related to the mean pressure $\sigma_r = p_m/\gamma_e$. Using Eq. (2), the representative strain is given by $\varepsilon_r = 1/(2\gamma_e(1-\nu^2))\tan(\beta)$. The value of γ_e being arbitrary, there is an infinite number of $(\sigma_r, \varepsilon_r)$ couples which give the correct value of the mean pressure.

Let us now consider elastic perfectly plastic materials. Both elastic and plastic deformations have to be taken into account. The representative strain is thus written $\varepsilon_r = \varepsilon_r^e + \varepsilon_r^p$. The elastic part is simply given by $\varepsilon_r^e = \sigma_r/E$. Similarly to the definition of Tabor [1], the representative plastic strain ε_r^p is considered to be strongly related to the shape of the indenter. Moreover ε_r^p must be equal to zero when the angle of the sharp indenter is not sufficient to produce plastic strain in the material. Therefore, we assume that ε_r^p can be written as:

$$\varepsilon_r^p = \left\langle \zeta\left(\tan(\beta) - \tan(\beta_0)\right)\right\rangle \tag{3}$$

where ζ is a parameter which will be defined below. $\langle\cdot\rangle$ represents the McCauley's bracket. β_0 is a critical angle introduced by Johnson [19] from which plastic deformations have to be taken into account. When $\beta \leqslant \beta_0$, the mean pressure is given by Eq. (2). β_0 depends on elastoplastic properties and is written

$$\tan(\beta_0) = B\frac{Y}{E} \tag{4}$$

where B equals to $\pi(1-\nu^2)/\sqrt{3}$ for a wedge and equals to $(1-\nu^2)$ for a cone. Theoretically, the infinite pressure at the apex will cause plastic flow even for $\beta \leqslant \beta_0$. Plastic deformation will take place but will be very small and confined to a small region close to the apex. As suggested by Johnson, such minor deformations should be neglected. In the sequel, we will consider that β is bigger than β_0 which implies that $\sigma_r = Y$.

The PGS being satisfied, the mean pressure does not depend on the contact radius and on the load applied on the indenter. Thus representative parameters can be defined. Let us define a linear elastic solid which gives the same representative stress and strain as those corresponding to the elastoplastic solid really indented. We will call it the representative elastic material and its Young's modulus will be given by $E_r = \sigma_r/\varepsilon_r$

$$E_r = \frac{Y}{Y/E + \zeta(\tan(\beta) - \tan(\beta_0))} \tag{5}$$

This material is fictitious and is only used to establish the approximate solution of the model.

For the representative elastic material, the value of $\gamma_e = p_m/\sigma_r$ is arbitrary. Let us choose γ_e equal to the ratio γ of the elastoplastic solid really indented. Hence the mean pressure obtained with the linear elastic solid is the same as that obtained with the elastic perfectly plastic solid. It is given by:

$$p_m = \frac{1}{2}\frac{E_r}{1-\nu_r^2}\tan(\beta) \tag{6}$$

where ν_r is the representative Poisson coefficient. Combining Eqs. (4) and (6), one obtains:

$$\gamma = \frac{p_m}{\sigma_r} = \frac{1}{2}\frac{1}{1-\nu_r^2}\frac{\tan(\beta)}{(1-\zeta B)Y/E + \zeta\tan(\beta)} \tag{7}$$

Eq. (7) must be valid for any elastic perfectly plastic solid. Let us consider the limit case of rigid perfectly plastic solids. For these solids $\gamma = \gamma_p$ depends only on β. Moreover the representative elastic strain is equal to zero ($Y/E = 0$). Eq. (7) then gives:

$$\zeta = \frac{1}{2\gamma_p}\frac{1}{1-\nu_r^2} \tag{8}$$

γ_p can be determined using the analysis of Hill [16] for wedge indentation and Lockett [17] for cone indentation.

Using an experimental approach, Tabor [1] suggests $\gamma_p = 3$. The last unknown factor relates to the expression of ν_r. To satisfy the limit case of elasticity, ν_r must be equal to ν. However, nothing indicates that ν_r does not depend on the mechanical properties of the material and in particular on the Y/E ratio. In his study of modelling the indentation of rigid plastic solids by non linear elastic solids, Hill [3] recommends a value of 0.5 for the Poisson coefficient in order to satisfy plastic incompressibility. Most engineering materials are more plastic than elastic during cone or wedge indentation tests, so we recommend $\nu_r = 0.5$. A simple illustration of these results is to consider γ_p equal to 3 and a rigid perfectly plastic solid $Y/E = 0$, $\nu_r = 0.5$. The expressions for σ_r and ε_r are:

$$\sigma_r = \frac{p_m}{3} \quad \text{and} \quad \varepsilon_r = 0.22\tan(\beta) \tag{9}$$

These expressions are very close to those suggested by Tabor [1] in the case of rigid plastic materials.

The main difficulty concerning the extension of this approach to work-hardening elastoplastic solids is that the $\gamma = p_m/\sigma_r$ ratio is not known in the case of rigid plastic solids. Storakers et al. [8], Larsson et al. [9] and Cheng and Cheng [4] have shown that when the work hardening is expressed as a power law written $\sigma = \sigma_0(\varepsilon^p)^{1/m}$ with σ_0 and m material constants and when the material considered is rigid plastic, the mean pressure is expressed as $p_m = B_1\sigma_0(B_2)^{1/m}$ in which B_1 and B_2 are constants. B_2 may be viewed as the representative plastic strain ε_r^p and B_1 as $\gamma = p_m/\sigma_r$. These results lead us to consider that γ for rigid plastic solids is constant and thus equals to γ_p. Hence Eq. (8) is still valid for work hardening plastic materials. For any elastoplastic material, the mean pressure is thus given by substituting Y with σ_r in Eqs. (7) developed previously for elastic perfectly plastic solids.

$$p_m = \frac{1}{2}\frac{1}{1-\nu_r^2}\frac{\sigma_r}{(1-\zeta B)\sigma_r/E + \zeta\tan(\beta)} \tag{10}$$

If the stress–strain curve of the material is known, then ε_r^p can be determined for any indentation tests using Eqs. (3), (4), (8) and (10). Then one obtains σ_r and thus the mean indentation pressure – or hardness – using Eq. (10).

3. Identification of the uniaxial stress–strain curve from indentation tests

A major interest of the indentation test is to obtain a $(\sigma_r, \varepsilon_r)$ couple related to the uniaxial stress–strain curve of the material. For each cone or wedge angle β, the quantities B and γ_p are known. ζ is given by Eq. (8) and ν_r equals to 0.5. Assuming that p_m and E are known – or can be measured experimentally – the representatives stress and strain can be computed using the following equations.

$$\sigma_r = \frac{\zeta\tan(\beta)p_m}{\gamma_p\zeta\tan(\beta) - (1-\zeta B)p_m/E} \tag{11}$$

$$\varepsilon_r = (1-\zeta B)\frac{\sigma_r}{E} + \zeta\tan(\beta) \tag{12}$$

With the development of the continuous stiffness measurement technique available on most nanoindentation devices [5,20], the contact K_c stiffness can be measured experimentally. This measure helps to determine the contact area and thus the mean pressure. If the elastic properties of the material are known, the determination is direct, otherwise special procedures must be used [5,20,12]. The measure of the mean indentation pressure gives one point on the uniaxial stress–strain curve. Consequently, the use of different cone or wedge angles β can be used to determine the uniaxial stress–strain curve of elastoplastic solids.

4. Numerical study

In this section, the results obtained above are verified using finite element simulations of indentation tests. Firstly, let us consider the model developed in Section 2 and particularly Eq. (10). Finite element simulations have been performed with 'Systus/Sysweld' [21] using an axisymmetric formulation to model cone indentation. In this study, the analysis is performed using a large displacement/large strain option. The plastic flow is described via a plastic von Mises criterion. In order to ensure plastic incompressibility, four node quadrilateral isoparametric elements with a selective reduced integration scheme are used in the plastically deformed area. The mesh is particularly fine near the contact zone, but it is also sufficiently wide to approximate a semi-infinite solid. For a good representation of the contact geometry, the width of the elements is determined in order to have at least 40 nodes in contact where the penetration is maximum. The height of the elements is about five times lower than the maximum penetration. The whole mesh contains about 9000 elements and 9400 nodes. The contact between the indenter and the workpiece is assumed to be frictionless and loading is achieved by monitoring quasi-static displacement of the indenter which is pushed vertically into the workpiece. The major difficulty is that the level of penetration has to reach a certain depth so as to minimize the error on the determination of the contact area and thus on the computation of the mean pressure [22].

Let us consider an elastic perfectly plastic material with a yield stress $Y = 100$ MPa. Several finite element calculations have also been performed with different values of the Young modulus from $E = 500$ MPa to $E = 30\,000$ MPa. For higher values of E, the mean pressure is approximatively constant. These values could correspond to those of some polymeric materials. The evolution of the mean indentation pressure p_m as a function of the Young modulus E has been studied for a cone angle $\beta = 10°$ in Fig. 1(left). The approximate model developed in this paper is plotted as a solid line. Based on the study of Lockett [17], we have chosen $\gamma_p = 3$ and $\nu_r = 0.5$ for this cone angle. Each numerical simulation gives a single point on Fig. 1(left). The agreement between the approximate model and the results of the numerical simulations is very satisfactory. The model developed by Johnson is also plotted but the results are less accurate than those obtained with the model proposed in this paper. An elastoplastic material which exhibits strain hardening has been studied. β is 20° and the values of γ_p and ν_r have been chosen at 2.8 and 0.5. The law of strain hardening follows a Ramberg–Osgood law – $\sigma = Y + K(\varepsilon^p)^n$ – with $Y = 100$ MPa, $K = 150$ MPa and $n = 0.5$. Several calculations have also been performed with different values of the Young modulus from $E = 500$ MPa to $E = 30\,000$ MPa. The evolution of the mean pressure p_m is plotted as a function of the Young modulus E on Fig. 1(right). As for the elastic perfectly plastic material the numerical results are in very good agreement with the approximation developed in Section 2.

Finally, the method developed in Section 3 is validated using finite element simulations. Let us consider the following materials: AISI304L [23] and heat treated AISI52100 [24]. The uniaxial stress–strain curve of these materials are an input parameter of the finite element simulations. Twenty numerical simulations corresponding to different values of β ($2° \leqslant \beta \leqslant 40°$) are performed. In this study, wedge indenters are used because the value of γ_p is known for each value of β (Hill [16]), which is not the case for cone indenters. Each numerical simulation gives the value of the mean indentation pressure. Then Eqs. (11) and (12) give σ_r and ε_r. For each material twenty different points $(\sigma_r; \varepsilon_r)$ are computed. The curve thus determined is compared to the real uniaxial stress–strain curve as well as the curve obtained with the Tabor method [1]. The results are plotted in Fig. 2.

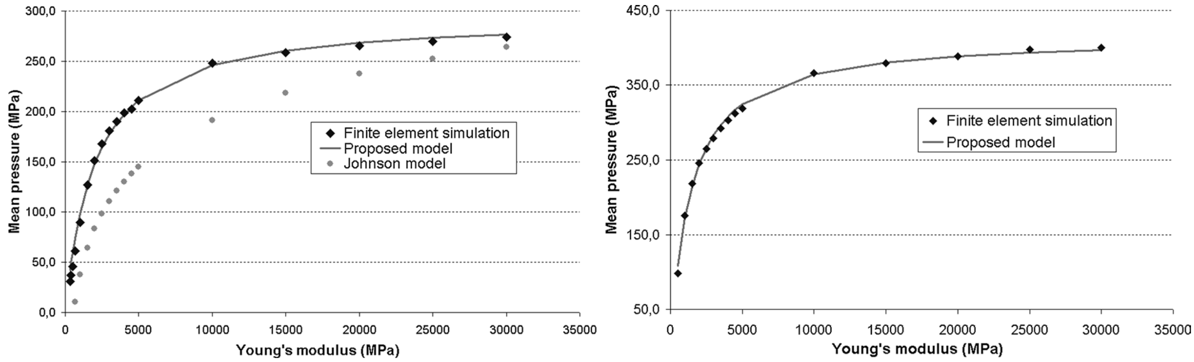

Fig. 1. Mean pressure versus Young's modulus; left: elastic perfectly plastic solids with $Y = 100$ MPa and $\beta = 10°$; right: work hardening elastoplastic solids with $Y = 100$ MPa, $K = 150$ MPa, $n = 0.5$ and $\beta = 20°$.
Fig. 1. Pression moyenne en fonction du module de Young ; à gauche: solides élastiques parfaitement plastiques avec $Y = 100$ MPa et $\beta = 10°$; à droite : solide élastoplastique écrouissable avec $Y = 100$ MPa, $K = 150$ MPa, $n = 0.5$ et $\beta = 20°$.

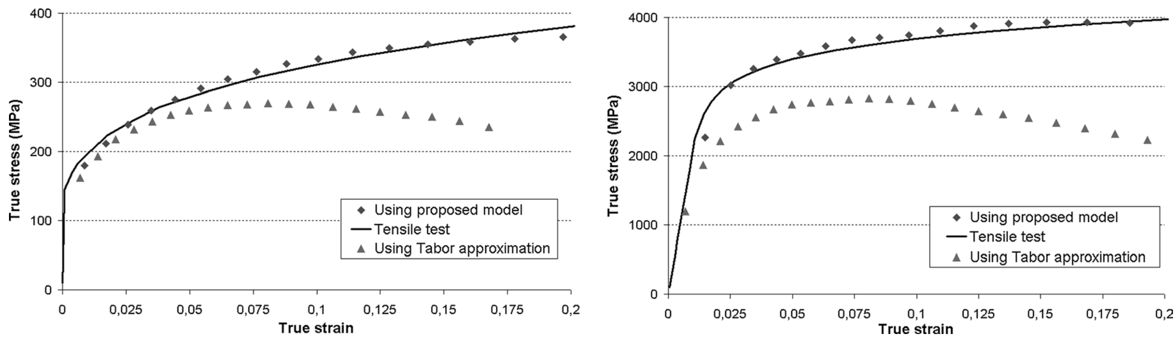

Fig. 2. Comparison of the stress strain curves obtained with the method proposed by Tabor, the present work and from tensile tests for the stainless AISI304L steel (left) and the AISI52100 heat treated steel (right).
Fig. 2. Comparaison des courbes contrainte-déformation obtenues à partir des méthodes d'identification de Tabor et celle proposée dans cette Note et à partir d'essais de traction pour l'acier inoxydable AISI304L (à gauche) et pour l'acier AISI52100 (à droite) traité thermiquement.

For both AISI304L stainless steel (Fig. 2 (left)) and heat treated AISI52100 steel (Fig. 2 (right)), the agreement between the rheology and the model developed in this study is very satisfactory. For AISI304L, Tabor's approximation seems to give correct results when the wedge angle is small. It comes from the fact that the deformation is mainly plastic, the solid can thus be considered as rigid plastic and γ_p is close to 3. In these conditions, the Tabor model can be used. For higher values of β, the approximation $\gamma_p = 3$ is no longer valid. It is the reason why this model does not give accurate results. For AISI52100 steel, Tabor's approximation does not work because the steel has been heat treated. Consequently the elastic deformation must be taken into account when compared to the plastic deformation. This model underestimates the representative stress and the representative strain. Contrary to the Tabor model the approximation developed in this Note gives results very close to the tensile curve of the two materials.

These numerical studies help to validate equations developed in Sections 2 and 3. Thanks to their simplicity, these expressions can be used easily with experimental indentation tests to convert hardness values into a representative stress and a representative strain. Identification methods based on dimensional analysis [4,12,14] give results equivalent to those obtained in this Note. The main advantage of the method proposed here is that it is easy to use and it does not require any approximation of the work hardening curve. Moreover, it does not call for intensive finite element calculations and can be easily and quickly adapted to other shapes of sharp indenters (Berkovitch, Vickers, Knoop, etc.).

References

[1] D. Tabor, The hardness of solids, J. Appl. Phys. (1971) 145–179.
[2] J.-L. Loubet, J.-M. Georges, G. Meille, Vickers indentation curves of elastoplastic materials, Microindentation Techniques in Mater. Sci. Engrg. (1986) 72–89.
[3] R. Hill, B. Storakers, A.-B. Zdunek, A theoretical study of the brinell hardness test, Proc. R. Soc. London Ser. A 423 (1989) 301–330.
[4] Y.-T. Cheng, C.-M. Cheng, Scaling, dimensional analysis, and indentation measurements, Mat. Sci. Engrg. 44 (2004) 91–149.
[5] W.-C. Oliver, G. Pharr, An improved technique for determining hardness and elastic modulus using load and displacement sensing indentation experiments, J. Mat. Res. 7 (1992) 1564–1583.
[6] S. Bec, A. Tonck, J.-M. Georges, E. Georges, J.-L. Loubet, Improvements in the indentation method with a surface force apparatus, Philos. Mag. A. 74 (1996) 1061–1072.
[7] R. Hill, Similarity analysis of creep indentation tests, Proc. R. Soc. London Ser. A 436 (1992) 617–630.
[8] B. Storakers, S. Biwa, P.L. Larsson, Similarity analysis of inelastic contact, Int. J. Solids Structures 34 (1997) 3061–3083.
[9] P.-L. Larsson, Investigation of sharp contact at rigid-plastic conditions, Int. J. Mat. Sci. 43 (2001) 895–920.
[10] K.-L. Johnson, The correlation of indentation experiments, J. Mech. Phys. Solids 18 (1970) 115–126.
[11] T.-A. Venkatesh, K.-J. Van Vliet, A.-E. Giannakopoulos, S. Suresh, Determination of elasto-plastic properties by instrumented sharp indentation: guidelines for property extraction, Scripta Mat. 42 (2000) 833–839.
[12] M. Dao, N. Chollacoop, K.-J. Van Vliet, T.-A. Ventakesh, S. Suresh, Computational modeling of the forward and reverse problems in instrumented sharp indentation, Acta Mat. 49 (2001) 3899–3918.
[13] M. Chollacoop, N. Dao, S. Suresh, Depth-sensing instrumented indentation with dual sharp indenters, Acta Mat. 51 (2002) 3713–3729.
[14] J.-L. Bucaille, S. Stauss, E. Felder, J. Michler, Determination of plastic properties of metals by instrumented indentation using different sharp indenters, Acta Mat. 447 (2003) 1663–1678.
[15] Y.-P. Cao, J. Lu, Depth-sensing instrumented indentation with dual sharp indenters: stability analysis and corresponding regularization schemes, Acta Mat. 52 (2004) 1143–1153.
[16] R. Hill, The Mathematical Theory of Plasticity, Oxford University Press, Oxford, 1950.
[17] F.-J. Lockett, Indentation of a rigid/plastic material by a conical indenter, J. Mech. Phys. Solids 11 (1963) 161–175.
[18] A.-E.-H. Love, Boussinesq's problem for a rigid cone, Quart. J. Math. 282 (1939) 161–175.
[19] K.-L. Johnson, Contact Mechanics, Cambridge University Press.
[20] J.-L. Loubet, M. Bauer, A. Tonck, S. Bec, B. Gauthier-Manuel, Nanoindentation with a surface force apparatus, Mechanical properties and deformation of materials having a ultra-fine microstructures (1993) 429–447.
[21] Systus/Sysweld, User's manual, ESI Group, 2004.
[22] T.-A. Laursen, J.-C. Simo, A study of the mechanics of microindentation using finite elements, J. Mat. Res. 7 (1992) 618–626.
[23] M. Barge, G. Kermouche, P. Gilles, J.-M. Bergheau, Experimental and numerical study of the ploughing part of abrasive wear, Wear 255 (2003) 30–37.
[24] G. Poulachon, Aspect phénoménologiques, mécaniques et métallurgiques en tournage c-BN des aciers durcis. Application à l'usinabilité de l'acier 100Cr6M, PhD Thesis, ENSAM, 1999.